ACS Medicinal Chemistry Letters

Letter

Synthesis, Cytotoxicity Evaluation and Computational Insights of Novel 1,4-Diazepane-Based Sigma Ligands

Daniele Zampieri, Sara Fortuna, Antonella Calabretti, Maurizio Romano, Renzo Menegazzi, Dirk Schepmann, Bernhard Wünsch, and Maria Grazia Mamolo

ACS Med. Chem. Lett., **Just Accepted Manuscript** • DOI: 10.1021/acsmedchemlett.9b00524 • Publication Date (Web): 16 Dec 2019

Synthesis, Cytotoxicity Evaluation and Computational Insights of Novel 1,4-Diazepane-Based Sigma Ligands

Daniele Zampieri[†*], Sara Fortuna[†], Antonella Calabretti[†], Maurizio Romano[¥], Renzo Menegazzi[¥], Dirk Schepmann[‡], Bernhard Wünsch[‡], and Maria Grazia Mamolo[†].

[†]Department of Chemical and Pharmaceutical Sciences, P.le Europa 1-Via Giorgieri 1, University of Trieste, 34127 Trieste, Italy.

[¥]Department of Life Sciences, Via Valerio 28/1, University of Trieste, 34127 Trieste, Italy.

[‡]Institute of Pharmaceutical and Medicinal Chemistry, Corrensstraße 48, 48149 Münster, Germany.

KEYWORDS. Sigma receptor, molecular dynamics, binding studies, cytotoxicity, antioxidant.

ABSTRACT: Among several potential applications, sigma receptors ligands can be used as antipsychotics, antiamnesic and against other neurodegenerative disorders as well as neuroprotective agents. We present herein a new series of diazepane-containing derivatives as σR ligands obtained by a conformational expansion approach of our previously synthesized piperidine-based compounds. The best results were reached by benzofurane **2c**, **3c** and quinoline **2d**, **3d** -substituted diazepane derivatives, which showed the highest σR affinity. The cytotoxic activities of synthesized compounds were evaluated against two cancer cell lines, and the results indicated that none of the compounds induced significant toxicity in these cells. We also evaluated the antioxidant activity by radical scavenging capacity of our best compounds on ABTS and H_2O_2. The results obtained reveal that our new derivatives possess an excellent antioxidant profile and could be protective for the cells. Overall, the benzofurane derivative **2c** due to its strong interaction with the active site of the receptor, as confirmed by molecular dynamic simulations, emerged as the optimum compound with high σ1R affinity, low cytotoxicity, and a potent antioxidant activity.

The sigma receptors (σ R) are a class of proteins initially classified, by Martin and coworkers,[1] as a subtype of the opiate receptors. Further studies revealed them to be a different receptor class comprising two distinct subtypes: σ 1 and σ 2.[2-5] The σ1R is a chaperone protein, cloned in 1996 from several tissues including human, consisting of 223 amino acids[6,7] with a MW of 25.3 kDa.[8] Crystallized twenty years later it revealed a trimeric protein organization.[9] The σ 1R subtype is primarily localized to mitochondria-associated ER membranes (MAM) of neuronal and peripheral cells, such as cardiac myocytes and hepatocytes. This receptor can also translocate to the plasma membrane or ER-membrane and regulate the activity of other proteins by modulating different ionic channels via an IP_3-indipendent mechanism.[10,11] The σ1Rs have neuroprotective and antiamnesic activity,[12,13] modulate opioid analgesia[14] as well as drug addiction,[15] and their antagonists seem to be effective against the negative manifestations of schizophrenia without producing extrapyramidal side effects.[16,17] In addition, several studies suggest a role for σ1R in tumor biology, since its expression increased in some cancers.[18]

After 40 years from the discovery of σRs,[1] in 2017, the σ2R subtype has been purified and identified as transmembrane protein-97 (TMEM97),[19] an endoplasmic-reticulum-resident transmembrane molecule implicated in cholesterol homeostasis due to its association with the lysosomal transporter NPC1.[20,21] The σ2R crystal structure is still elusive, but several pharmacophore models have been proposed.[22-25]

The σ2Rs are overexpressed in many cancer cell lines including lung cancer,[26,27] breast cancer,[28] ovarian cancer,[29] glioma cancer[30] and gastric cancer.[31] In this context, since σ2R agonists can induce tumor cell death, they have been proposed as potential antitumor drugs. On the other hand, the σ2Rs are widely expressed in cerebellum, red nucleus, and substantia nigra, and are a potential target for the treatment of movement disorders and of neuroleptic-induced acute dystonia.[32] In addition, σ1R antagonists as well as σ2R agonists can modulate neuropathic pain.[33,34]

In the last decade, our group has synthesized and biologically evaluated an extensive series of compounds both of preferential affinity for σ1R and σ2R subtypes. Following up our studies in this field, we report herein the development of a new class of sigma ligands designed through the expansion of the conformational selection paradigm applied to our previously synthesized piperidine-based σ1R ligands **1** (Figure 1).[35]

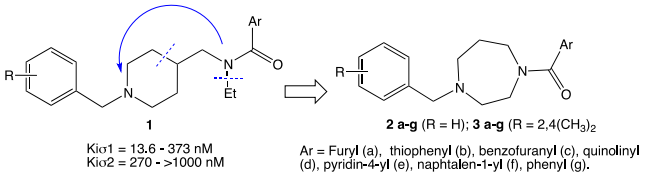

Figure 1. Conformational expansion approach starting from previously synthesized sigma ligands **1**.

In addition to the spacer replacement, we opted to expand the new series of compounds by using various aromatic fragments, including heterocycles, both monocycles and bicycles, linked to the amide carbonyl group. Moreover, in order to verify the influence on the sigma affinity of the substitution on benzyl moiety, we decided to retain the unsubstituted phenyl ring, present in many σ1R ligands and the 2,4-dimethyl substituted phenyl ring, typical of several σ2R ligands.[36] The synthesis of our new diazepane-based derivatives **2a-g** and **3a-g** is depicted in Scheme 1.

The synthetic route of our new series of compounds (Supporting information) was carried out by treating the appropriate, commercially available, 1-benzyl-1,4-diazepane, which was made to react with the appropriate aroyl chloride to give the corresponding first subseries **2a-g**. These compounds did not need further purification after the classical work-up. The 2,4-dimethyl derivatives **3a-g** were obtained in three reaction steps, starting from 1-Boc-1,4-diazepane and the corresponding aroyl chloride to provide the acylated intermediates **4a-g**. The cleavage of protecting N-Boc group with TFA, led to the intermediates **5a-g** which were subsequently N-alkylated, with a direct reductive amination using 2,4-dimetylbenzaldheyde and $NaCNBH_3$, to give the final subseries **3a-g**. These compounds were purified by DCVC technique.

Scheme 1. Synthesis of compounds 2a-g and 3a-g[a]

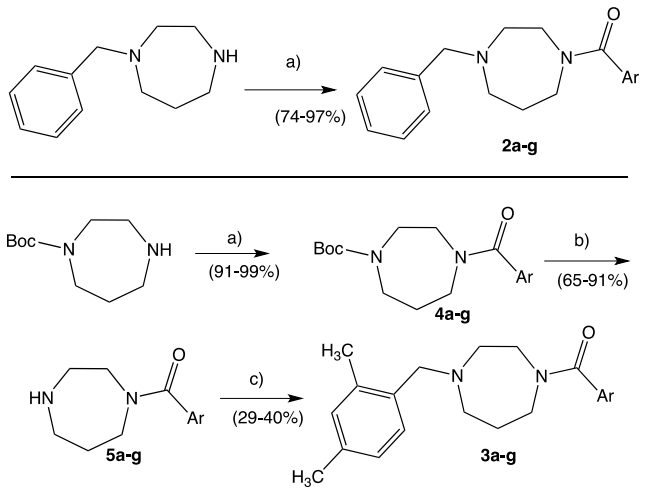

[a]a) DCM, Et_3N, 0°C; b) DCM, TFA, rt; c) DCM, 2,4-dimethylbenzaldheyde, $NaCNBH_3$ rt.

The σ1R and σ2R affinities of the test compounds were determined in competition experiments by radiometric assays, using [^{3}H]-(+)-Pentazocine as radioligand for the σ1R assay, and [^{3}H]-DTG (di-*o*-tolylguanidine) as radioligand in the σ2R assay. Compounds **2a-g** and **3a-g** were tested against σ1R and σ2R of animal origin, prepared from guinea pig brain and rat liver membranes by homogenization, centrifugation and washing of the respective tissues. We also performed a competition experiment towards GluN2b subunit containing NMDA receptors in a radioligand binding assay. This receptor subtype plays important roles in synaptic transmission and plasticity, learning, memory and other physiological and pathological processes.[37,38] Hence, antagonist of GluN2b subunit are of interest as neuroprotective drugs for various CNS disorders. The radioligand used in the competition assay was [^{3}H]-labeled Ifenprodil, a prototypical allosteric inhibitor of GluN2b subunit (Supporting Information).

For compounds with affinity value higher than 100 nM, only one measure was performed. The σ1R, σ2R and GluN2b affinities of compounds **2a-g** and **3a-g** are presented in Table 1.

Table 1. Affinities of compounds 2a-g and 3a-g towards σ1, σ2 and GluN2b receptors.

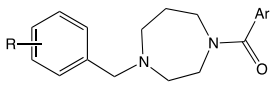

Cmpd	R	Ar	K_i (nM)[a]		
			σ1	σ2	GluN2b
2a	H		333	560	1 %
2b			147	297	0 %
2c			8.0 ± 0.6	47 ± 15	1.6 μM
2d			19 ± 3.2	47 ± 19	1.5 μM
2e			267	495	0 %
2f			41 ± 12	187	9 %
2g			116	0 %	0 %
3a	$2,4(CH_3)_2$		690	3.9 μM	0 %
3b			336	1.8 μM	3 %
3c			20 ± 5	28 ± 11	59 ± 12
3d			29±10	35±4	108
3e			254	2 μM	116
3f			70 ± 7	102	79 ± 19
3g			849	3.9 μM	294
Ifp	-	-	125 ± 24	98 ± 34	10 ± 7.0
Hal	-	-	6.3 ± 1.6	78 ± 2.3	nt[b]
DTG	-	-	89 ± 29	57 ± 18	nt

[a]Only compounds with highest affinities (<100 nM) were tested in triplicates. For low-affinity compounds, the competition curves were recorded only once (single value), whereas the inhibition of the radioligand binding (shown as %) was assayed at a test compound concentration of 1 μM; [b]not tested.

From the obtained data we can summarize the following: i) the bulky diazepane spacer retained, or even improved, the σR affinity to both σ1 and σ2, with respect to piperidine ring; ii) only bicycle derivatives displayed moderate to high affinity towards both σR subtypes, while the corresponding monocycles analogues were weak inhibitors or avoiding of σR affinity; iii) the best results against σ1R was reached by benzofurane derivative **2c**, while its 2,4-dimethyl substituted analogue **3c** gave the best pan-affinity with K_i values of 8.0 and 28 nM towards both σR subtypes and also the best GluN2b inhibition value of 59 nM; iv) the 2,4-dimethyl substitution on benzyl moiety derivatives, improves the σ2 over σ1 affinity of the bicycle derivatives, as well as the affinity towards GluN2b subunit receptor.

To get insight the interaction of our compounds into the σ1R active site, we performed a computational assessment of the best σ1R ligand of the series, **2c**, in comparison with its monocycle analogue **2a**.

We prepared the σ1R following our previously procedure[36] (Supporting information) and we docked compounds **2a** and **2c** to the target by following the same protocol.

The comparison between the optimum pose obtained for each compound (Figure 2) suggests that compound **2c** slides further into the pocket than **2a** pushing its benzene ring to interact with Trp164 and Phe133, closed at the bottom by Tyr206, and forming an H-bond with Thr181. Moreover, compound **2c** optimum pose is predicted to be in touch through 17 hydrophobic interactions with target residues and a hydrogen bond with Thr181 (inset in Figure 2a). Also compound **2a** interacts with the target with 17 hydrophobic interactions including Thr181 and shares 14 of those interactions with compound **2c** (inset in Figure 2b).

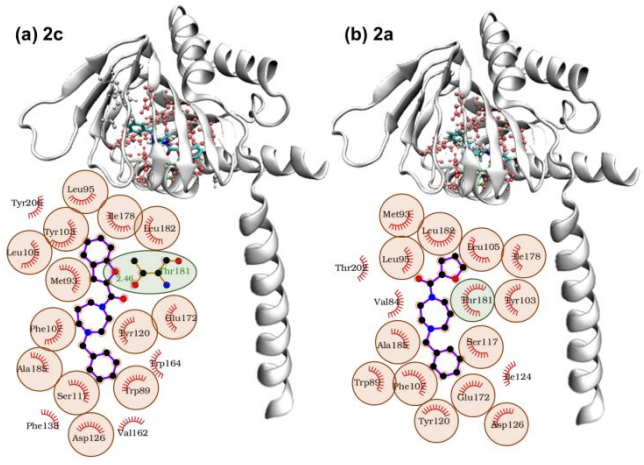

Figure 2. 3D putative of (a) compound **2c** and (b) compound **2a** in the optimum AutoDock pose. Protein residues interacting with both compounds by van der Waals interactions are highlighted in red, Thr 181 in green, other interacting residues (Trp 164, Phe 133, Tyr 206 in panel (a) and Thr202, Val84, Ile124 in panel (b)) are white. In the insets: schematic diagrams of the interaction between the receptor and the respective compounds in the same optimum AutoDock pose. Protein residues interacting with the compounds by van der Waals interactions are highlighted in red, while hydrogen bonds are indicated by green dotted lines. The hydrogen bonds distances are also indicated. Residues interacting with both compounds through van der Waals interactions are circled in red. Thr 181 (circled in green) form a hydrophobic interaction with compounds **2a**, while a hydrogen bond with compound **2c**.

To confirm the docking result and understand the different behavior of the two compounds we ran 250 ns of molecular dynamics (MD) simulation of the complexes in water solvent. The ligand topologies were built with ATB.[39] The topologies were validated as the molecular mechanics minimized structure of compound **2a** had root mean square deviation (RMSD) of 0.01007 nm with respect to the semi-empirical minimized structure, while for compound **2c** the same RMSD was 0.0082 nm.

The trajectories, scored with the Autodock Vina scoring function,[40] showed a constant binding score for both compounds (Figure 3a,b). For both systems the protein backbone RMSD diverged along the dynamics up to 0.6 nm (Figure 3c,d), as expected by simulating only a monomer of the extracellular domain. The ligands RMSD with respect to the fixed protein backbone, below 0.4 nm for compound **2c** (Figure 3c), revealed a major conformational change for compound **2a** (RMSD > 1.0 nm, Figure 3d). These variations were not reflected in the protein backbone radius of gyration constant at 1.6 nm for both systems (Figure 3e,f). Larger protein rearrangements peaks at residues 190-200 for both systems, as observed in the protein backbone root mean square fluctuation (RMSF > 0.5 nm, Figure 3g,h). These are part of the helical structure delimitating the pocket but not directly interacting with the ligands (Figure 3i,j and insets in Figure 2). Along the whole simulated time ligands were not observed to leave the pocket with compound **2c** maintaining its position but rotating its benzene ring (Figure 3i) and compound **2a** changing position by both flipping its orientation and further sliding inside the pocket (Figure 3j), a movement not associated with a gain in binding energy as calculated by Autodock Vina score (Figure 3b).

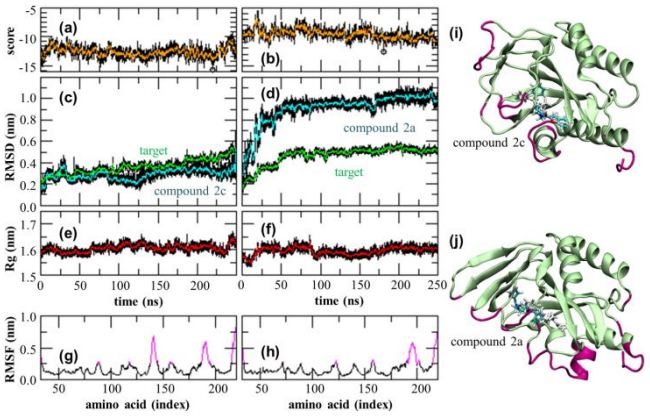

Figure 3. Molecular dynamics simulations analysis for compound **2c** (left column) and **2a** (right column): (a,b) Autodock Vina score, (c,d) protein backbone RMSD (green) and ligands RMSD in the protein backbone frame (blue), (e,f) protein backbone radius of gyration,(g,h) protein backbone RMSF with values above 0.25 nm highlighted in magenta. All values measured with respect to the starting configuration correspond to the minimized optimum pose identified by docking. Simulation snapshots taken at the lowest Autodock Vina score (circled in panels a,b) for (i) compound **2c** and (j) compound **2a**. Protein residues with RMSF

above 0.25 nm are highlighted (magenta). The starting ligand configuration is also indicated (white).

The MM/PBSA analysis confirmed that the van der Waals interactions were the major liable for binding the compounds, a contribution that is more relevant for compound **2c** which also benefits of a less unfavorable polar solvation energy than that calculated for compound **2a** (Figure 4a,b). This result is reflected by the single amino acid contribution to the binding energy. Indeed, for compound **2a** several amino acids opposed to the binding with Arg119 and Glu172 contribution larger than 1 kcal/mol, followed by Gln135, Asp126, and His154. Instead, compound **2c** is synergistically kept bound to its interacting site by several residues (Figure 4d). More in details (Figure 4e,f) there are seven residues (namely Leu105, Ile124, Phe107, Trp89, Val84, Leu182, and Tyr103) contributing to the binding energy with more than 0.9 kcal/mol with the major contributing force to be ascribed to van der Waals forces and hydrophobic interactions.

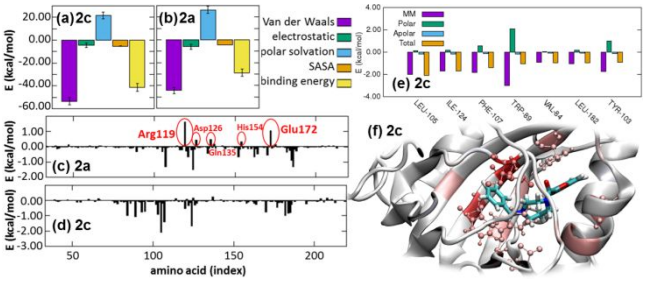

Figure 4. MMPBSA analysis: energetic contributions to the receptor binding of (a) compound **2c**, and (b) compound **2a**, and amino acids contribution to the total binding energy of (c) compound **2a**, and (d) compound **2c** with highlighted the amino acids opposing to the binding with predicted energy larger than 0.3 kcal/mol; (e) details of the contributions of each amino acid with binding energy larger than 0.9 kcal/mol for compound **2c**; (f) snapshot of the complex σ1/**2c** with highlighted amino acids (shades of red) contributing to the binding energy with more than ± 0.9 kcal/mol. All data averaged over the last 150 ns of the molecular dynamics trajectory.

Overall the larger ring keeps the ligand fixed in its position, which is more accessible to Thr181 for H-bonding. A larger number of contacts deep into the pocket further inhibited the molecular rearrangement inside the protein pocket.

The effects of this new set of σ1R ligands on cell health were evaluated by testing the cytotoxic response of the human pancreatic carcinoma (PANC1) and human neuroblastoma (SH-SY5Y) cell lines, selected because they express high levels of σ1R.[18] To this aim, we selected the most interesting compounds (**2c**, **2d**, **3c** and **3d)** and tested their potential toxicity by MTT assay (Supporting information, Table S1 and Table S2). The experiments revealed that none of our diazepane-containing derivatives showed significant cytotoxicity at different concentrations, with the exception of compound **3d** which exhibited a moderate toxicity toward PANC1 cells, but only at 100 μM concentration (viability of 51%). Interestingly, compounds **2c** and **2d**, which exhibited the best σ1R affinities (K_i = 8 and 19 nM, respectively), resulted to be the less toxic (viability: 127 and 196% at 50 μM; 98 and 127% at 100 μM, in SH-SY5Y and PANC1, respectively). Therefore, considering the general consensus that σ1R agonists promote cell survival,[41,42] these results support the hypothesis that compounds **2c**, **2d**, **3c** and **3d,** can be included in this category.

Motivated by these results, we evaluated the *in vitro* antioxidant activity of the same compounds tested in the aforementioned cytotoxic assay. We tested the ability to scavenge ABTS derived radicals and H_2O_2 oxidant. Ascorbic acid and Trolox (6-hydroxy-2,5,7,8-tetramethylchroman-2-carboxylic acid) were used as standard antioxidants in comparison test. The assayed compounds potently inhibited ABTS radicals and H_2O_2, compared to the standards (Table 2).

Table 2. *In vitro* antioxidant activity of compounds 2c, 2d, 3c and 3d.

Cmpd	IC_{50} (μg/mL)[a]	
	ABTS	H_2O_2
2c	12.71 ± 0.25	15.89 ± 0.18
2d	14.26 ± 0.15	20.35 ± 0.27
3c	10.05 ± 0.09	18.56 ± 0.31
3d	9.43 ± 0.11	17.44 ± 0.18
Ascorbic Acid	12.75 ± 0.12	19.27 ± 0.54
Trolox	18.73 ± 0.26	20.38 ± 0.19

[a]All measurements were performed in triplicate

Among the series, the dimethyl substituted compounds **3c** and **3d** exhibited a significant radical scavenging capacity on both ABTS and H_2O_2 with values of 10.05 and 18.56 μM/mL for **3c** and 9.43 and 17.44 μM/mL for **3d**, lower than compared standards, ascorbic acid and Trolox (12.75, 19.27 μM/mL and 18.73, 20.38 μM/mL, respectively).

Furthermore, in order to evaluate their drug likeness and the potential ability to cross the BBB, the compounds **2a-g** and **3a-g** were also *in-silico* scored for their physiochemical and pharmacokinetic parameters (ADME) by using the extended version of Lipinski's rule of five. All the compounds were found to be BBB permeant and none of them violate any Lipinski's RO5 (Supporting information).

In conclusion, we have synthesized a new series of ring-expanded diazepane-based compounds. The new series showed enhanced affinity than its original counterpart[35] towards both σR subtypes and, among the series, the benzofurane derivative **2c** showed the best σ1R affinity and molecular dynamic simulations confirmed a strong interaction with the active site of the receptor. The benzofurane and quinoline derivatives **2c**, **3c** and **2d, 3d**, displayed the best K_iσ values and a safe profile towards two human cell lines. Altogether these data, along with the documented radical scavenging and cell survival promoting activities, support the interest for further studies aiming at evaluating the potential neuroprotective activity of this novel series of σ1R ligands.

ASSOCIATED CONTENT

Supporting Information

The Supporting Information is available free of charge on the ACS Publications website.

Detailed experimental, synthetic procedures and characterization of compounds, additional computational details, pharmacology and cytotoxicity assays, antioxidant activity, drug likeness prediction (PDF).

AUTHOR INFORMATION

Corresponding Author

* Daniele Zampieri; tel. +390405587858; dzampieri@units.it

Author Contributions

DZ synthesized and characterized the compounds and wrote the manuscript; SF generated the computational results and analysis; AC performed the antioxidant assay; MR and RM tested the cytotoxicity of the compounds and wrote the manuscript; DS and BW performed the binding assay; DZ and MGM conceived the project. The manuscript was written through contributions of all authors. All authors have given approval to the final version of the manuscript.

Notes

The authors declare no competing financial interest.

ACKNOWLEDGMENT

We thank Dr. Fabio Hollan (University of Trieste, DSCF) for the MS data. We acknowledge the CINECA Awards N. HP10CKYM0P, 2019, for the availability of high performance computing resources and support.

ABBREVIATIONS

σ1R and σ2R, sigma-1 and sigma-2 receptor; ABTS, 2,2'-azino-bis(3-ethylbenzothiazoline-6-sulphonic acid; ADME, absorption distribution metabolism excretion; ATB, automated topology builder; BBB, blood brain barrier; Boc, *tert*-butyloxycarbonyl; CNS, central nervous system; DCM, dichloromethane; DCVC, direct column vacuum chromatography; DTG, di-*o*-tolylguanidine; Et_3N, triethylamine; ER, endoplasmatic reticulum; DMEM, Dulbecco's Modified Eagle's Medium; MAM, mitochondrion-associated membrane; MD, molecular dynamics; MMPBSA, molecular mechanics Poisson-Boltzmann surface area; MW, molecular weight; NMDA, N-methyl-D-aspartic acid; NPC1, Niemann-Pick cholesterol transporter type1; RMSD, root mean square deviation; RMSF root mean squared fluctuation; RO5, rule of five; TLC, thin-layer chromatography; TFA, trifluoroacetic acid; TMEM97, transmembrane protein-97;

REFERENCES

(1) Martin, W.R.; Eades, C.E.; Thompson, J.A.; Huppler, R.E.; Gilbert, P.E. The effects of morphine- and nalorphine- like drugs in the nondependent and morphine-dependent chronic spinal dog. *J. Pharmacol. Exp. Ther.* **1976**, *197*, 517-532.

(2) Su, T.-P. Evidence for sigma opioid receptor: binding of [3H]SKF-10047 to etorphine-inaccessible sites in guinea-pig brain. *J. Pharmacol. Exp. Ther.* **1982**, *223,* 284–290.

(3) Quirion, R.; Bowen, W.D.; Itzhak, Y.; Junien, J.L.; Musacchio, J.M.; Rothman, R.B.; Su, T.-P.; Tam S.W.; Taylor, D.P. A proposal for the classification of sigma binding sites *Trends Pharmacol. Sci.* **1992**, *13*, 85–86.

(4) Walker, J.M.; Bowen, W.D.; Goldstein, S.R.; Roberts, A.H.; Patrick, S.L.; Hohmann, A.G.; DeCosta, B. Autoradiographic distribution of [3H](+)-pentazocine and [3H]1,3-di-o-tolylguanidine (DTG) binding sites in guinea pig brain: a comparative study, *Brain Res.* **1992**, *581*, 33–38.

(5) Bouchard, P.; Quirion, R. [3H]1,3-di(2-tolyl)guanidine and [3H](+)pentazocine binding sites in the rat brain: autoradiographic visualization of the putative sigma1 sigma2 receptor subtypes, *Neuroscience* **1997**, *76*, 467–477.

(6) Hanner, M.; Moebius, F.F.; Flandorfer, A.; Knaus, H.G.; Striessnig, J.; Kempner, E.; Glossmann, H. Purification, molecular cloning, and expression of the mammalian sigma1-binding site. *Proc. Natl. Acad. Sci.* U.S.A. **1996**, *93*, 8072-8077.

(7) Kekuda, R.; Prasad, P.D.; Fei, Y.J.; Leibach, F.H.; Ganapathy, V. Cloning and functional expression of the human type 1 sigma receptor (hSigmaR1). *Biochem. Biophys. Res. Commun.* **1996**, *229*, 553−558.

(8) Hellewell, S.B.; Bruce, A.; Feinstein, G.; Orringer, J.; Williams, W.; Bowen, W.D. Rat liver and kidney contain high densities of σ1 and 2 receptors: characterization by ligand binding and photoaffinity labeling, *Eur. J. Pharmacol., Mol. Pharmacol. Sect.* **1994**, *268*, 9−18.

(9) Schmidt, H.R.; Zheng, S.; Gurpinar, E.; Koehl, A.; Manglik, A.; Kruse, A.C. Crystal structure of the human σ1 receptor, *Nature* **2016**, *532*, 527−530.

(10) Hayashy, T.; Su, T.-P. Regulating ankyrin dynamics: Roles of sigma-1 receptors, *Proc. Natl. Acad. Sci.* U. S. A. **2001**, *98*, 491-496.

(11) Wu, Z.; Bowen, W.D. Role of sigma-1 receptor C-terminal segment in inositol 1,4,5-trisphosphate receptor activation: constitutive enhancement of calcium signaling in MCF-7 tumor cells, *J. Biol. Chem*. **2008**, *283*, 28198-28215.

(12) Cobos, E.J.; Entrena, J.M.; Nieto, F.R.; Cendan, C.M.; Pozo, E.D. Pharmacology and therapeutic potential of sigma-1 ligands, *Curr. Neuropharmocol.* **2008**, *6*, 344-366.].

(13) Maurice, T.; Lockhart, B.P. Neuroprotective and anti-amnesic potentials of sigma (sigma) receptor ligands, *Prog. Neuropsychopharmacol. Biol. Psychiatry.* **1997**, *21*, 69-102.

(14) King, M.; Pan, Y.X.; Mei, J.; Chang, A.; Xu, J.; Pasternak, G.W.; Enhanced kappa-opioid receptor-mediated analgesia by antisense targeting the sigma1 receptor, *Eur. J. Pharmacol*. **1997**, *331*, (1997) R5-6.

(15) McCracken, K.A.; Bowen, W.D.; Walker, F.O.; De Costa, B.; Matsumoto, R.R.; Two novel sigma receptor ligands, BD1047 and LR172, attenuate cocaine-induced toxicity and locomotor activity, *Eur. J. Pharmacol.* **1999**, *370*, 225-232.

(16) Modell, S.; Nober, D.; Holzbach, R. Efficacy and safety of an opiate sigma-receptor antagonist (SL 82.0715) in schizophrenic patients with negative symptoms: an open dose-range study, *Pharmacopsychiatry* **1996**, *29*, 63-66.

(17) Huber, M.T.; Gotthardt, U.; Schreiber, W.; Krieg, J.C. Efficacy and safety of the sigma receptor ligand EMD 57445 (panamesine) in patients with schizophrenia: an open clinical trial, *Pharmacopsychiatry* **1999**, *32*, 68-72.

(18) Kim, F.J.; Maher, C.M. *Sigma1 Pharmacology in the Context of Cancer.* Handbook of Experimental Pharmacology: Springer, 2017, pp 237-308.

(19) Alon, A.; Schmidt, H.R.; Wood, M.D.; Sahn, J.J.; Martin, S.F.; Kruse, A.C. Identification of the gene that codes for the σ2 receptor, *Proc. Nat. Ac. Sc.* **2017**, *114*, 7160–7165.

(20) Bartz, F.; Kern, L.; Erz, D.; Zhu, M.; Gilbert, D.; Meinhof, T.; Wirkner, U.; Erfle, H.; Muckenthaler, M.; Pepperkok, R.; Runz, H. Identification of cholesterol-regulating genes by targeted RNAi screening, *Cell. Metab.* **2009**, *10*, 63-75.

(21) Riad, A.; Zeng, C.; Weng, C.C.; Winters, H.; Xu, K.; Makvandi, M.; Metz, T.; Carlin, S.; Mach, R.H. Sigma-2 Receptor/TMEM97 and PGRMC-1 Increase the Rate of Internalization of LDL by LDL Receptor through the formation of a Ternary Complex, *Sc. Rep.* **2018**, *8*, 16845.

(22) Cratteri, P.; Romanelli, M.N.; Cruciani, G.; Bonaccini, C.; Melani, F. Grind-derived pharmacopore model for a series of alfa-trophanyl derivative ligands of the sigma-2 receptor, *J. Comuput. Aided Mol. Des.* **2004**, *18*, 361-374.

(23) Laurini, E.; Zampieri, D.; Mamolo, M.G.; Vio, L.; Zanette, C.; Florio, C.; Posocco, P.; Fermeglia, M.; Pricl, S. A 3D-Pharmacophore model for σ2 receptors based on a series of substituted benzo[d]oxazol-2(3H)-one derivatives. *Bioorg. Med. Chem. Lett.* **2010**, *20*, 2954-2957.

(24) Rhoades, D.J.; Kinder, D.H.; Mahfouz, T.M. A Comprehensive Ligand Based Mapping of the 2 Receptor Binding Pocket. *Med. Chem.* **2014**, *10*, 98-121.

(25) Foresta, G.; Rescifina, A.; Marrazzo A.; Dichiara, M.; Pistarà, V.; Pittalà, V.; Prezzavento, O.; Amata, E. Hyphenated 3D-QSAR statistical model-scaffold hopping analysis for the identification of potentially potent and selective sigma-2 receptor ligands. *Eur. J. Med. Chem.* **2017**, *139*, 884-891.

(26) Han K.Y.; Gu, X.; Wang, H.R.; Liu, D.; Lv, F.Z.; Li, J.N. Overexpression of MAC30 is associated with poor clinical outcome in human non-small cell lung cancer, *Tumour Biol.* **2013**, *34*, 821-825.

(27) Ding, H.; Gui, X.H.; Lin, X.B.; Chen, R.H.; Cai, H.R.; Fen, Y.; Sheng, Y.L. Prognostic value of MAC30 expression in human pure squamous cell carcinomas of the lung, *Asian Pac. J. Cancer Prev.* **2016**, *17*, 2705-2710.

(28) Xiao, M.; Li, H.; Yang, S.; Huang, Y.; Jia, S.; Wang, H.; Wang, J.; Li, Z. Expression of MAC30 protein is related to survival and clinicopathological variables in breast cancer, *J. Surg. Oncol.* **2013**, *107*, 456-462.

(29) Yang, S.; Li, H.; Liu, Y.; Ning, X.; Meng, F.; Xiao, M.; Wang, D.; Lou, G.; Zhang, Y. Elevated expression of MAC30 predicts lymph node metastasis and unfavourable prognosis in patients with epithelial ovarian cancer, *Med. Oncol.* **2013**, *30*, 324.

(30) Qiu, G.; Sun, W.; Zou, Y.; Cai, Z.; Wang, P.; Lin, X.; Huang, J.; Jiang, L.; Ding, X.; Hu, G.RNA interference against TMEM97 inhibits cell proliferation, migration, and invasion in glioma cells, *Tumour Biol.* **2015**, *36*, 8231-8238.

(31) Xu, X.Y.; Zhang, L.J.; Yu, Y.Q.; Zhang, X.T.; Huang, W.J.; Nie, X.C.; Song, G.Q. Downregulated MAC30 expression inhibits proliferation and mobility of human gastric cancer cells, *Cell. Physiol. Biochem.* **2014**, *33*, 1359-1368.

(32) Rousseaux C.G.; Greene, S.F., Sigma receptors [σRs]: biology in normal and diseased states. *J. Recept. Signal Transduct Res.* **2016**, *36,* 327–388.

(33) Zamanillo, D.; Romero, L.; Merlos, M.; Vela, J.M., Sigma 1 receptor: a new therapeutic target for pain. *Eur. J. Pharmacol.* **2013**, *716*, 78−93.

(34) Sahn, J.J.; Mejia, G.L.; Ray, P.R.; Martin, S.F.; Price, T.J., Sigma 2 Receptor/Tmem97 Agonists Produce Long Lasting Antineuropathic Pain Effects in Mice", *ACS Chem. Neurosci.* **2017**, *8*, 1801-1811.

(35) Zampieri, D.; Laurini, E.; Vio, L.; Golob, S.; Fermeglia, M.; Pricl, S.; Mamolo, M.G. Synthesis and receptor binding studies of some new arylcarboxamide derivative as sigma-1 ligands. *Bioorg. Med. Chem. Lett.* **2014**, *24,* 1021-1025.

(36) Zampieri, D.; Fortuna, S.; Calabretti, A.; Romano, M.; Menegazzi, R.; Schepmann, D.; Wünsch, B.; Collina, S.; Zanon, D.; Mamolo, M.G. Discovery of new potent dual sigma receptor/GluN2b ligands with antioxidant property as neuroprotective agents. *Eur. J. Med. Chem.* **2019**, *180,* 268-282.

(37) Riedel, G.; Platt, B.; Micheau, J. Glutamate receptor function in learning and memory. *Behav. Brain Res.* **2003**, *140*, 1-47.

(38) Paoletti, P..; Bellone, C.; Zhou, Q. NMDA receptor subunit diversity: impact on receptor properties, synaptic plasticity and disease. *Nat. Rev. Neurosci.* **2013**, *14,* 383-400.

(39) Malde, A.K., Zuo, L.; Breeze, M.; Stroet, M.; Poger, D.; Nair, P.C.; Oostenbrink, C.; Mark A.E. An Automated Force Field Topology Builder (ATB) and Repository: Version 1.0. *J. Chem. Theory and Comput.* **2011**, *7,* 4026-4037.

(40) Trott, O.; Olson A.J., AutoDock Vina: improving the speed and accuracy of docking with a new scoring function, efficient optimization, and multithreading. *J. Comput. Chem.* **2010**, *31*, 455-461.

(41) Maurice, T.; Su, T.P., The pharmacology of sigma-1 receptors, *Pharmacol. Ther.* **2009** *124*, 195-206.

(42) Hayashi, T.; Su, T.P., Sigma-1 receptor chaperones at the ER-mitochondrion interface regulate Ca(2+) signaling and cell survival. *Cell*, **2007**, *131*, 596-610.

Insert Table of Contents artwork here

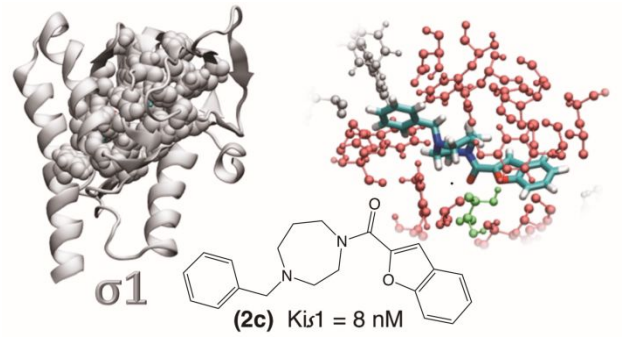

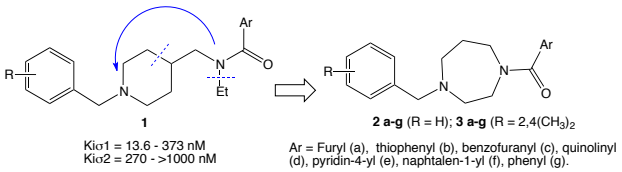

Figure 1. Conformational expansion approach starting from previously synthesized sigma ligands **1**.

Scheme 1. Synthesis of compounds 2a-g and 3a-g[a]

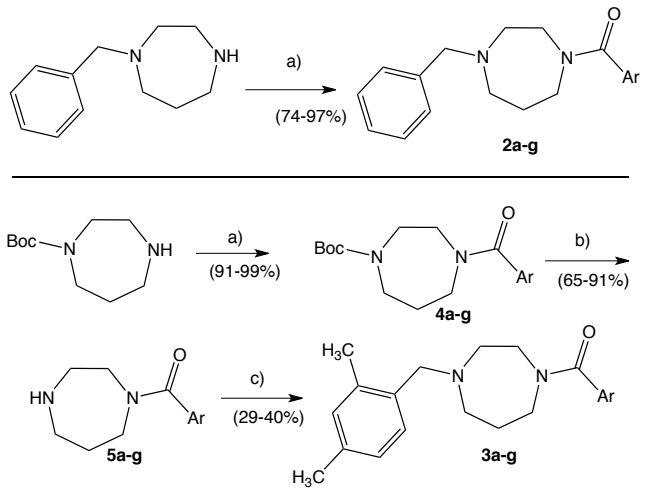

[a]a) DCM, Et_3N, 0°C; b) DCM, TFA, rt; c) DCM, 2,4-dimethylbenzaldheyde, $NaCNBH_3$ rt.

Table 1. Affinities of compounds 2a-g and 3a-g towards σ1, σ2 and GluN2b receptors.

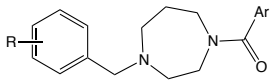

Cmpd	R	Ar	K_i (nM) [a]		
			σ1	σ2	GluN2b
2a	H		333	560	1 %
2b			147	297	0 %
2c			8.0 ± 0.6	47 ± 15	1.6 μM
2d			19 ± 3.2	47 ± 19	1.5 μM
2e			267	495	0 %
2f			41 ± 12	187	9 %
2g			116	0 %	0 %
3a	$2,4(CH_3)_2$		690	3.9 μM	0 %
3b			336	1.8 μM	3 %
3c			20 ± 5	28 ± 11	59 ± 12
3d			29±10	35±4	108
3e			254	2 μM	116
3f			70 ± 7	102	79 ± 19
3g			849	3.9 μM	294
Ifp	-	-	125 ± 24	98 ± 34	10 ± 7.0
Hal	-	-	6.3 ± 1.6	78 ± 2.3	nt[b]
DTG	-	-	89 ± 29	57 ± 18	nt

[a]Only compounds with highest affinities (<100 nM) were tested in triplicates. For low-affinity compounds, the competition curves were recorded only once (single value), whereas the inhibition of the radioligand binding (shown as %) was assayed at a test compound concentration of 1 μM; [b]not tested.

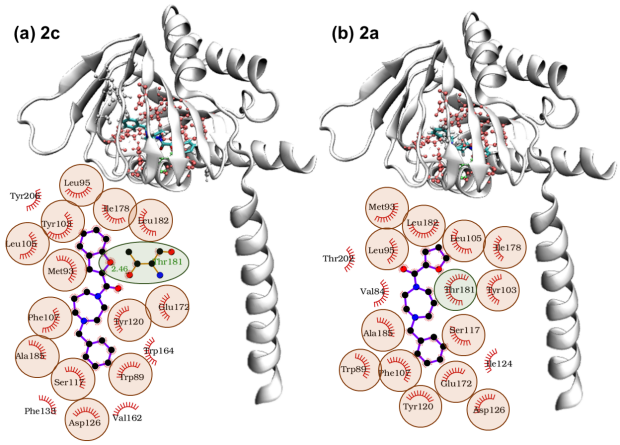

Figure 2. 3D putative of (a) compound **2c** and (b) compound **2a** in the optimum AutoDock pose. Protein residues interacting with both compounds by van der Waals interactions are highlighted in red, Thr 181 in green, other interacting residues (Trp 164, Phe 133, Tyr 206 in panel (a) and Thr202, Val84, Ile124 in panel (b)) are white. In the insets: schematic diagrams of the interaction between the receptor and the respective compounds in the same optimum AutoDock pose. Protein residues interacting with the compounds by van der Waals interactions are highlighted in red, while hydrogen bonds are indicated by green dotted lines. The hydrogen bonds distances are also indicated. Residues interacting with both compounds through van der Waals interactions are circled in red. Thr 181 (circled in green) form a hydrophobic interaction with compounds **2a**, while a hydrogen bond with compound **2c**.

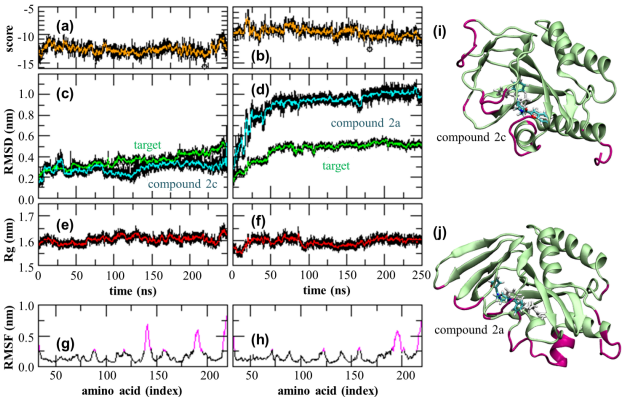

Figure 3. Molecular dynamics simulations analysis for compound **2c** (left column) and **2a** (right column): (a,b) Autodock Vina score, (c,d) protein backbone RMSD (green) and ligands RMSD in the protein backbone frame (blue), (e,f) protein backbone radius of gyration,(g,h) protein backbone RMSF with values above 0.25 nm highlighted in magenta. All values measured with respect to the starting configuration correspond to the minimized optimum pose identified by docking. Simulation snapshots taken at the lowest Autodock Vina score (circled in panels a,b) for (i) compound **2c** and (j) compound **2a**. Protein residues with RMSF above 0.25 nm are highlighted (magenta). The starting ligand configuration is also indicated (white).

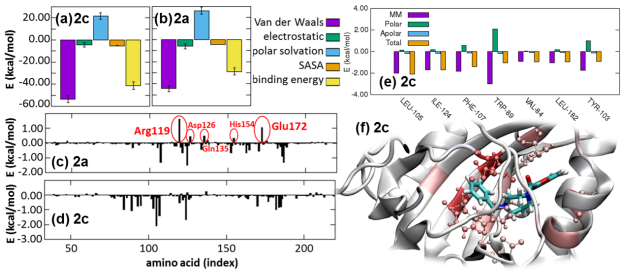

Figure 4. MMPBSA analysis: energetic contributions to the receptor binding of (a) compound **2c**, and (b) compound **2a**, and amino acids contribution to the total binding energy of (c) compound **2a**, and (d) compound **2c** with highlighted the amino acids opposing to the binding with predicted energy larger than 0.3 kcal/mol; (e) details of the contributions of each amino acid with binding energy larger than 0.9 kcal/mol for compound **2c**; (f) snapshot of the complex σ1/**2c** with highlighted amino acids (shades of red) contributing to the binding energy with more than ± 0.9 kcal/mol. All data averaged over the last 150 ns of the molecular dynamics trajectory.

Table 2. *In vitro* antioxidant activity of compounds 2c, 2d, 3c and 3d.

Cmpd	IC_{50} (μg/mL)[a]	
	ABTS	H_2O_2
2c	12.71 ± 0.25	15.89 ± 0.18
2d	14.26 ± 0.15	20.35 ± 0.27
3c	10.05 ± 0.09	18.56 ± 0.31
3d	9.43 ± 0.11	17.44 ± 0.18
Ascorbic Acid	12.75 ± 0.12	19.27 ± 0.54
Trolox	18.73 ± 0.26	20.38 ± 0.19

[a]All measurements were performed in triplicate